Parametric resonance in a spin-1/2 chain: dynamical effects of nontrivial topology

Mahmoud T. Elewa¹ and M. I. Dykman¹

¹Department of Physics and Astronomy, Michigan State University, East Lansing, Michigan 48824 (Dated: November 17, 2025)

Resonant parametric modulation is a major tool of studying magnetic systems. For a spin-1/2 chain in a strong magnetic field, the resulting excitations can be mapped on fermionic excitations in the Kitaev chain. We show that the response to the modulation turn-on allows one to reveal dynamical aspects of the nontrivial topology of the periodic chain. In the topological regime, depending on how fast the turn-on is, the system displays the absence of spatial magnetization correlations or their increase with the increasing detuning of the modulation from resonance. The transition between the topological and trivial regimes is controlled by the modulation frequency.

Sufficiently strong periodic modulation of magnetic systems can lead to parametric excitation of magnons [1]. Various aspects of this effect have been broadly studied. Recent examples range from the Bose-Einstein condensation away from thermal equilibrium [2, 3] to dynamical demagnetization [4], non-equilibrium topological magnon edge current [5], induced magnon-magnon coupling [6], magnonic turbulence [7], and magnon-magnon entanglement and quantum magnonics [8]. Magnons are bosonic excitations; they are usually described by applying the Holstein-Primakoff or Villain transformations [9, 10] to large-spin systems.

Here we are interested in parametric modulation of spin-1/2 chains. Excitations in such chains are mapped on spinless fermions [11, 12]. A remarkable feature of chains of spinless fermions discovered by Kitaev [13] is that, in the presence of pairing coupling, the system becomes topologically nontrivial. Much of the previous work on the manifestations of this feature in spin-1/2 chains driven by periodic fields was centered at the edge modes, cf. Refs. [14–20] and references therein. The analysis focused primarily on modulation by periodic rectangular pulses. Such modulation is often implemented in quantum simulations, in particular.

In the present paper we consider resonant parametric excitation of spin-1/2 chains. Such excitation may lead to strong effects even where the modulating field is comparatively weak. Similar to magnons, if the modulation is long-wavelength, excitations in a translationally-symmetric system should be created in pairs with opposite wave vectors \mathbf{k} and $-\mathbf{k}$. The modulation should be most efficient if its frequency is close to the sum of the excitation frequencies. A resonantly modulated spin chain in a strong magnetic field was mapped on the Kitaev chain and the onset of nontrivial topology was indicated in Ref. [21]. The modulation has been implemented and some of its consequences explored in systems of up to six transmon qubits that mimicked coupled spins [22].

In contrast to studies focusing on topological edgestate effects, in this paper we study how the Kitaevchain topology affects *bulk* properties of a modulated spin chain. Respectively, we consider closed spin chains. We find profound bulk topological effects. The topology is controlled by the modulation frequency. The state of the

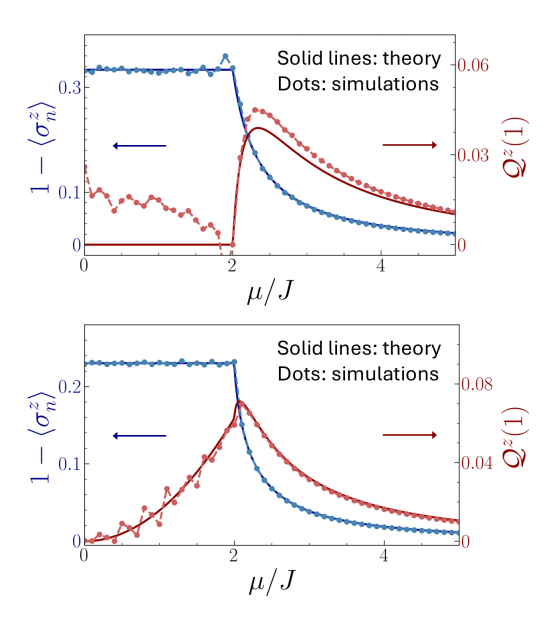


FIG. 1. The time-averaged excitation density, $1-\langle \sigma_n^z \rangle$, and the nearest-neighbor correlator $\mathcal{Q}^z(1)=\langle \sigma_n^z \sigma_{n+1}^z \rangle - \langle \sigma_n^z \rangle^2$ in a modulated closed spin chain as functions of the detuning of the modulation frequency μ scaled by the hopping integral J. The upper and lower panels refer to the sudden and quasi-adiabatic modulation turn-on. The matrix-product-state simulations refer to the chain periods N=20 and N=40, respectively. The final modulation amplitude is $F(t_f)=J/2$. The slow turn-on regime in the simulations was implemented using $F(t)=F(t_f)t/\tau_{\rm sl}$ with $\tau_{\rm sl}=10^3/J$.

system after the modulation is turned on is qualitatively different depending on whether the modulation frequency lies in the topologically trivial or nontrivial regime. The state also strongly depends on whether the modulation is turned on fast or slowly, as seen in Fig. 1.

We consider a periodic N-spin chain in a strong magnetic field with nearest-neighbor anisotropic XY coupling. Resonant parametric excitation comes from sinusoidally modulating the coupling at frequency ω_F close to twice the Larmor frequency ω_0 . The Hamiltonian of

the chain is

$$\hat{H}_{0} = -\frac{1}{2}\omega_{0} \sum_{n=1}^{N} \sigma_{n}^{z} - J_{xx}(t) \sum_{n=1}^{N} \sigma_{n}^{x} \sigma_{n+1}^{x} - J_{yy} \sum_{n=1}^{N} \sigma_{n}^{y} \sigma_{n+1}^{y},$$

$$J_{xx}(t) = \bar{J}_{xx} + 2F \cos(\omega_{F}t), \qquad (\hbar = 1), \qquad (1)$$

where σ_n^i are the Pauli matrices $(i = \{x, y, z\})$ and F is the modulation amplitude. We assume that the coupling parameters and the modulation amplitude are small compared to ω_0 . Then it is convenient to go to the rotating frame at frequency $\omega_F/2$ using the standard transformation $U = \exp[i(\omega_F t/4) \sum_n \sigma_n^z]$. In the rotating wave approximation the Hamiltonian becomes

$$\hat{H}_{\text{RWA}} = \frac{1}{2} \mu \sum_{n=1}^{N} \sigma_n^z - J \sum_{n=1}^{N} (\sigma_n^+ \sigma_{n+1}^- + \sigma_{n+1}^+ \sigma_n^-)$$

$$- F \sum_{n=1}^{N} (\sigma_n^+ \sigma_{n+1}^+ + \sigma_{n+1}^- \sigma_n^-), \quad \mu = \frac{1}{2} \omega_F - \omega_0, \quad (2)$$

where $J = \bar{J}_{xx} + J_{yy}$, μ is the detuning of the modulation frequency from the exact resonance, and $\sigma_n^{\pm} = (\sigma_n^x \pm i\sigma_n^y)/2$. The parameters μ , J, and F are generally of the same order of magnitude. It is seen from Eq. (2) that the parametric modulation corresponds to flipping a pair of spins, reminiscent of creating a pair of magnons.

The spin chain (2) naturally maps by the Jordan-Wigner transformation [11, 12] on the Kitaev chain of spinless fermions. In particular, the parametric-modulation term maps on the term of the pairing interaction. This suggests that the modulation leads to a nontrivial topology of the spin chain. We will analyze it for periodic boundary conditions with even N. The Hamiltonian of the Fourier-transformed fermions in the Nambu form reads

$$\hat{H} = -\frac{1}{2} \sum_{k} \vec{c}_{k}^{\dagger} (M_{k} \tau^{z} + F_{k} \tau^{x}) \vec{c}_{k},$$

$$M_{k} = \mu - 2J \cos k, \quad F_{k} = 2F \sin k$$
(3)

Here c_k and c_k^{\dagger} are the creation and annihilation operators of the fermions, $\vec{c}_k = \begin{pmatrix} c_k \\ c_{-k}^{\dagger} \end{pmatrix}$, $\tau^{x,z}$ are the Paulimatrices, and $-\pi < k \le \pi$ [23]. It is well-known from the Kitaev chain theory that the range $|\mu/J| > 2$ corresponds to a topologically trivial regime, whereas for $|\mu/J| < 2$ the system of fermions, and thus the resonantly modulated spin chain, are topologically nontrivial.

The Hamiltonian (3) provides a convenient way to study the effect of turning on parametric modulation in the trivial and topological regimes. We will consider this effect assuming that, in the laboratory frame, in the initial state $|\Psi_0\rangle$ the spins are polarized along the strong magnetic field, $\langle \Psi_0 | \sigma_n^z | \Psi_0 \rangle = 1$. In terms of the fermions, $|\Psi_0\rangle$ is the vacuum of the c_k -operators, $c_k |\Psi_0\rangle = 0$. It is an eigenstate of \hat{H} for F = 0. We will

consider expectation values of the operators that commute with the parity operator $\prod_n \sigma_n^z$.

The state $|\Psi_0\rangle$ is not an eigenstate of \hat{H} for nonzero F. Therefore, turning on modulation leads to a complicated time evolution of the wave function. We will be interested in the long-time behavior of physical observables of the spin chain, which is determined by the time-averaged expectation values of the spin-chain operators and their spatial correlators, such as

$$1 - \langle \sigma_n^z \rangle = \frac{2}{N} \sum_k \langle c_k^{\dagger} c_k \rangle, \quad \mathcal{Q}^z(m) = \langle \Delta \sigma_n^z \Delta \sigma_{n+m}^z \rangle$$
$$= \frac{4}{N^2} \sum_{k_1, \dots, k_4} \langle c_{k_1}^{\dagger} c_{k_2} c_{k_3}^{\dagger} c_{k_4} \rangle e^{i(k_1 - k_2)m} \delta_{k_1 - k_2, k_4 - k_3}. \quad (4)$$

Here $\Delta \sigma_n^z = \sigma_n^z - \langle \sigma_n^z \rangle$. We use $\langle \cdot \rangle$ to indicate the time-averaged expectation value,

$$\langle A \rangle = T^{-1} \int_{t_f}^{t_f + T} \langle \Psi_0 | A(t) | \Psi_0 \rangle, \qquad (5)$$

where A(t) is an operator in the Heisenberg representation and t_f is the time by which the modulation reaches its final value. Spin observables appear to depend strongly on how quickly the modulation is turned on.

Rapid turn-on of the modulation. We will first assume that the modulation is sharply switched on at t=0, increasing from F=0 to a finite F over time δt such that $\omega_0^{-1} \ll \delta t = t_f \ll |J|^{-1}$. The Hamiltonian \hat{H} for |F| > 0 is diagonalized by the fermionic operators d_k, d_k^{\dagger} ,

$$d_k = c_k \cos(\theta_k/2) + c_{-k}^{\dagger} \sin(\theta_k/2), \quad \tan \theta_k = F_k/M_k.$$

$$\varepsilon_k = (M_k^2 + F_k^2)^{1/2}.$$
(6)

The values of ε_k here give the eigenvalues of \hat{H} ; in the Heisenberg representation $d_k(t) = \exp(iHt)d_k\exp(-iHt) = d_k(0)\exp[i\varepsilon_kt \operatorname{sgn}(M_k\cos\theta_k)]$. We set θ_k to be a continuous function of k; in particular, $M_k\cos\theta_k$ has the same sign for $M_k\to +0$ and $M_k\to -0$.

The time-averaged expectation values of spin correlators can be calculated in 2 steps. First, using Eq. (6) one finds the expectation values on the state $|\Psi_0\rangle$ of the pairs $d_k^{\dagger}d_k$, d_kd_{-k} , and $d_k^{\dagger}d_{-k}^{\dagger}$ (pairs with nonzero total momentum are not excited). Only a contribution from the terms $\langle \Psi_0 | d_k^{\dagger}(t) d_k(t) | \Psi_0 \rangle$ "survives" averaging over time for $T \gg [\min \varepsilon_k(t_f)]^{-1}$. We then express, again from Eq. (6), the averages $\langle c_k^{\dagger}c_k \rangle$, $\langle c_kc_{-k} \rangle$, and $\langle c_k^{\dagger}c_{-k}^{\dagger} \rangle$ in terms of $\langle d_k^{\dagger}d_k \rangle$, which ultimately expresses the averages in terms of θ_k . For example, $\langle c_k^{\dagger}c_k \rangle = \frac{1}{2}\sin^2\theta_k$. This gives the spin correlators in terms of θ_k .

The nontrivial topology manifests when summation (integration) over k is performed. This is a consequence of the structure of the Hamiltonian \hat{H} . In particular, from Eq. (6), the winding number of the chain is $\nu = (2\pi)^{-1} \int_{-\pi}^{\pi} dk (d\theta_k/dk) = -\Theta(1 - |\mu/2J|) \operatorname{sgn}(FJ)$,

where $\Theta(x)$ is the step function. In other words, as k goes over the Brillouin zone, θ_k is incremented by $\pm 2\pi$ in the topologically nontrivial range $|\mu/2J| < 1$, whereas it returns to the initial value in the trivial regime. We note that the sign of F can be changed at the transition to the rotating frame by incrementing $t \to t + \pi/\omega_F$. Therefore of physical significance is $|\nu|$. We note also that different winding numbers emerge in models with direct 3-spin coupling [24, 25].

To illustrate how the topology affects spins we will first consider the correlator $Q^z(m)$. The calculation is similar to the calculation $\int dk (d\theta/dk)$. Changing from integration over k to integration over the unit circles |w|=1 with $w=\exp(ik)$ or $w=\exp(-ik)$ [23], after some algebra we obtain from Eqs. (4) and (6)

$$Q^{z}(m) = \sum_{\alpha=1,2} (-1)^{\alpha} |q_{\alpha}(m)|^{2}, \qquad q_{\alpha}(m) = (F/4\pi)$$

$$\times \operatorname{Im} \oint dw \, w^{|m|-1} (w^{2} - 1) [P_{1}^{-1}(w) - (-1)^{\alpha} P_{2}^{-1}(w)],$$

$$P_{\beta}(w) = F(w^{2} - 1) - (-1)^{\beta} [\mu w - J(w^{2} + 1)] \quad (\beta = 1, 2)$$
(7)

In the range $|\mu/2J| < 1$, where the system is topologically nontrivial, $P_1(w)$ has no roots with |w| < 1 for FJ > 0, whereas $P_2(w)$ has no such roots for FJ < 0. Therefore, from Eq. (7), the time-averaged pair correlation function of the z-components of the spins is zero. Moreover, higher-order correlators are zero, too [23]. Zero time-averaged correlations of σ_n^z are a "bulk" manifestation of the nontrivial topology of the spin chain. In the trivial regime both $P_1(w)$ and $P_2(w)$ have one root with |w| < 1, and then $Q^z(m)$ is nonzero. From Eqs. (6) and (7), the structure of $P_{1,2}(w)$ determines also the value of the winding number.

Figure 1 shows the dependence of the correlator $Q^z(1)$ on μ , i.e., on the modulation frequency. For $|\mu| > 2|J|$, the correlator first sharply increases with the increasing $|\mu|$, and then falls off. The fall-off corresponds to the halved modulation frequency moving away from the Larmor frequency, and thus from resonance. Since the integrands in Eq. (7) have a factor $w^{|m|-1}$, where w is given by the pole inside the circle |w|=1, the pair correlators quickly fall-off with the increasing |m|. Higher-order spin correlators display a similar dependence on μ and the interspin distance [23].

Figure 1 also shows the mean spin polarization $\langle \sigma_n^z \rangle = 1 - 2N^{-1} \sum_k \langle c_k^{\dagger} c_k \rangle$ as a function of μ . A change of $\langle \sigma_n^z \rangle$ is a conventional manifestation of parametric excitation. In the considered case it can be calculated in the same way as $\mathcal{Q}^z(m)$. Depending on the sign of FJ, it is conveniently expressed in term of a contour integral over $w = \exp(ik)$ or $w = \exp(-ik)$ that contains only P_1^{-1} or P_2^{-1} , giving

$$1 - \langle \sigma_n^z \rangle = (1 + |J/F|)^{-1}, \quad |\mu/2J| < 1.$$

Thus, the effect of parametric modulation is independent of the modulation frequency. Outside the topo-

logical regime, the magnetization falls off with the increasing $|\mu|$, with $1-\langle\sigma_n^z\rangle\propto\mu^{-2}$ for large $|\mu|$ [23]. In the interesting paper [26] it was found that, for the Kitaev chain, if the pairing coupling is suddenly turned on, $(i/N)\sum_{k>0}\langle c_{-k}c_k-c_k^{\dagger}c_{-k}^{\dagger}\rangle$ is independent of μ in the topological regime. This correlator does not contribute to $\langle\sigma_n^z\rangle$ and its relation to the nonzero winding number was not discussed.

Other spin correlators, besides Q^z , also display nontrivial behavior. In particular, $\langle \sigma_n^+ \sigma_{n+1}^- \rangle = -N^{-1} \sum_k \langle c_k^\dagger c_k \rangle \cos k \to -[\mu \operatorname{sgn}(JF)/4F](1+|J/F|)^{-2}$ in the topological regime, i.e., the correlator linearly increases with $|\mu|$. For large $|\mu|$ it falls off as $1/|\mu|$. This behavior is shown in Fig. 2. The theory is in excellent agreement with the matrix product state (MPS) simulations already for N=20, except for $Q^z(1)$. This is a consequence of the non-Wick contribution to the simulated $Q^z(1)$ from the terms, which are quartic in the fermionic operators; this contribution gives a correction $\propto 1/N$ for a finite chain [23].

We note that our results refer not only to spin, but also to qubit systems. For the both systems the time-averaged parameters can be directly measured in the experiment using conventional measurement techniques, cf. [27, 28].

Slow turn-on of the modulation. The nontrivial topology also strongly affects the outcome of a slow turn-on of parametric excitation of a spin chain. We will assume that the modulation is increased from F(t) = 0 for t = 0 to a certain value $F(t_f)$ at time t_f and is not changed afterwards. We will consider the state of the chain for $t > t_f$ and, again, will be interested in the time-averaged chain parameters, so that transients will have decayed.

Fermionic excitations of the chain are created pairwise with zero total momentum. The evolution of a fermion pair (k, -k) is described by coupled Heisenberg equations for the operators d_k , d_{-k}^{\dagger} , which follow from Eqs. (3) - (6),

$$\dot{d}_k = i\varepsilon_k d_k + \frac{1}{2}\dot{\theta}_k d_{-k}^{\dagger}, \quad \dot{d}_{-k}^{\dagger} = -i\varepsilon_k d_{-k}^{\dagger} - \frac{1}{2}\dot{\theta}_k d_k. \quad (8)$$

Here $\varepsilon_k \equiv \varepsilon_k(t)$ is given by Eq. (6) with $F \equiv F(t)$. Equation (8) is written for $M_k \cos \theta_k > 0$. This parameter does not change sign with varying F(t); if $M_k \cos \theta_k < 0$ one should replace $\varepsilon_k \to -\varepsilon_k$ in Eq. (8).

It is easy to solve Eq. (8) in the adiabatic approximation, where we disregard the term $\propto \dot{\theta}_k \propto \dot{F}_k$. This gives $d_k(t) = d_k(0) \exp[i \int_0^t dt' \varepsilon_k(t')]$. Of interest for the time-averaged spin chain parameters are the expectation values $\langle d_k^{\dagger}(t) d_k(t) \rangle$. From Eq. (6) we have

$$\langle d_k^{\dagger}(t)d_k(t)\rangle = \langle \Psi_0| d_k^{\dagger}(0)d_k(0) |\Psi_0\rangle = \sin^2[\theta_k(0)/2], (9)$$

where we took into account that $c_k | \Psi_0 \rangle = 0$. Equation (6) also shows that the rotation angle $\theta_k(0)$ is either 0 or π for F = 0. Then, as the modulation amplitude increases, $\theta_k(t)$ is seen from Eq. (6) to vary, respectively, within the range $(-\pi/2, \pi/2)$ or $(\pi/2, 3\pi/2)$, reaching the corresponding $\theta(t_f)$ once F(t) reaches its stationary value

 $F(t_f)$. The value of $\theta(t_f)$ gives the relation between the operators $d_k(t)$ and $c_k(t)$ for $t > t_f$.

From Eq. (9) we obtain $\langle c_k^{\dagger}(t)c_k(t)\rangle = [\varepsilon_k(t_f) - |M_k|]/2\varepsilon_k(t_f)$ and $\langle c_k(t)c_{-k}(t)\rangle = [F_k(t_f)/2\varepsilon_k(t_f)] \mathrm{sgn}(M_k)$. These expressions allow us to find in the explicit form both $\langle \sigma_n^z \rangle$ and the spin correlators, as it was done earlier for quench. Again, the result depends on the singularities encountered in the contour integrals over $w = \exp(\pm ik)$, as in the case of the winding number, except that here the singularities are branching points rather than poles.

Interestingly, there are similarities in the dependence of the spin parameters on the drive frequency in the adiabatic and sudden turn-on regimes. In particular, as seen from Fig. 1, in the both regimes $\langle \sigma_n^z \rangle$ is independent of μ in the topologically nontrivial range $|\mu/2J|<1$ and falls off with the increasing $|\mu|$ for $|\mu/2J|>1$. The results for the spin correlators $\langle \sigma_n^+\sigma_{n+1}^-\rangle$ are shown in Fig. 2. These correlators linearly depend on μ in the topological regime. However, for the adiabatic turn-on, the correlators $\langle \sigma_n^z\sigma_{n+1}^z\rangle$ do not vanish in the topological regime, in contrast to the sudden turn-on of the modulation.

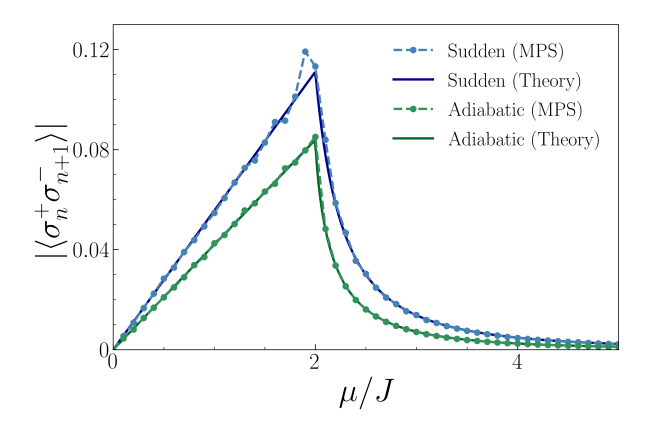


FIG. 2. The time-averaged correlators $|\langle \sigma_n^+ \sigma_{n+1}^- \rangle| = -\langle \sigma_n^+ \sigma_{n+1}^- \rangle$ for slow and sudden turn-on of parametric modulation as functions of the scaled frequency detuning μ/J . The results refer to the final modulation amplitude $F(t_f)/J=0.5$. The simulations of the sudden and slow turn-on refer to N=20 and N=40, respectively. The slow turn-on was implemented using $F(t)=F(t_f)t/\tau_{\rm sl}$ with $\tau_{\rm sl}=10^3/J$.

The adiabaticity condition $|\theta_k| \ll \varepsilon_k$ breaks down in the topological regime $|\mu/2J| < 1$ when the drive is still weak. This is because, for F = 0, we have $\varepsilon_k = 0$ for $k = \pm k_\mu$ with $k_\mu = \arccos(\mu/2J)$. Therefore, excitations are unavoidably generated as F is turned on. From Eq. (6) for θ_k we see that the adiabatic approximation does not apply for F = 0 and $||k| - k_\mu| \lesssim |\dot{F}/G_\mu|^{1/2}$, where $G_\mu = J(4J^2 - \mu^2)^{1/2}$. The resulting nonadiabatic corrections to the expressions for the spin correlators and $\langle \sigma_n^z \rangle$ are proportional to the size of the corresponding range of k and thus scale as $|\dot{F}/G_\mu|^{1/2}$. They increase as the system approaches the critical value of the modulation frequency where $|\mu/2J| = 1$. For $|\mu/2J| = 1$ the width

of the nonadiabatic region scales as $(|\dot{F}|/J^2)^{1/3}$.

The energy gap closing at $|\mu/2J|=1$ and k=0 or $k=\pi$ persists for all values of F(t). This leads to corrections to time-averaged spin correlators. In particular, in the sudden turn-on approximation, we disregarded the time-averaged matrix elements $[d_k(t)d_{-k}(t)+\mathrm{H.c.}]$, which are $\propto \sin(2\varepsilon_k T)/2\varepsilon_k T$. At criticality, since $\varepsilon_k \approx 2|F(t_f)k|$ for $|k| \ll 1$, the resulting correction is $\sim 1/F(t_f)T$, where $F(t_f)$ is the amplitude of the switched-on field. The smallness of this correction is determined by the restriction on T imposed by the spin relaxation and the $\sigma_n^z \sigma_m^z$ coupling disregarded in our model.

Both in the sudden and the adiabatic approximations, the derivatives of $\langle \sigma_n^z \rangle$ and the time-averaged spin correlators over μ are discontinuous at criticality, $\mu=\pm 2J$. This is seen in Figs. 1 and 2. Such behavior is a consequence of the energy gap closing in the thermodynamic limit and the winding number changing discontinuously.

Hysteresis. The different dynamics in the trivial and nontrivial regime lead to a memory effect illustrated in Fig. 3. One can bring the system to a state with the same value of F and μ (with $|\mu/2J| < 1$) in different ways. First, one can slowly switch on the drive for a given $\mu = \mu_0$ in the topological regime. Second, one can switch on the drive in the trivial regime and then slowly change μ to bring it to μ_0 . As μ crosses the critical value $\pm 2J$, the adiabatic approximation breaks down via the Kibble-Zurek mechanism, cf. [29–33]. However, for a slowly varying μ the resulting change of the time-averaged spin correlators is small. The large difference between the values of the correlators in Fig. 3 (see also [23]) points to a strong memory effect: the system "remembers" how it was brought to a given state.

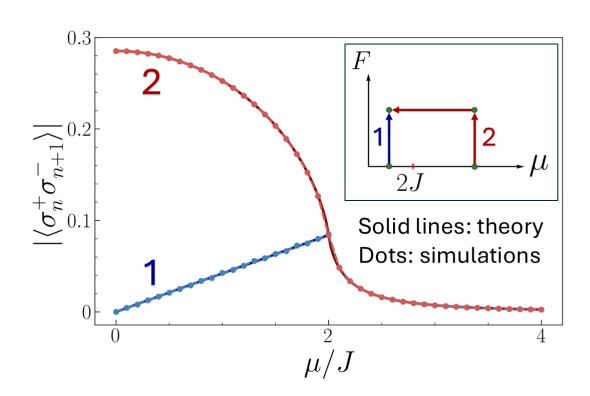


FIG. 3. The time-averaged correlators $|\langle \sigma_n^+ \sigma_{n+1}^- \rangle| = -\langle \sigma_n^+ \sigma_{n+1}^- \rangle$ obtained by slowly increasing the drive to $F(t_f)/J = 0.5$ for a fixed μ (line and circles 1) and by slowly turning on the drive to the same F/J in the trivial regime and then slowly changing the modulation frequency to arrive at the same μ (line and circles 2). The simulations refer to N=40 and $F(t)=F(t_f)t/\tau_{\rm sl}$ with $\tau_{\rm sl}=10^3/J$.

For a slowly turned-on drive, $|\dot{\varepsilon}_k| \ll \varepsilon_k^2$, the Schrödinger equation for the fermion wave function can be solved in the WKB approximation. For a linear ramp of F(t), the general solution is given by the parabolic

cylinder functions for arbitrary $\dot{\varepsilon}_k/\varepsilon_k^2$; the WKB solution can be matched to it, providing a complete description of the dynamics for a slowly turned-on drive [23]. We note that, for $k = k_{\mu}$, the correlators $\langle c_k^{\dagger} c_k \rangle$ and $\langle c_k c_{-k} \rangle$ can be found for an arbitrary protocol of switching F(t).

This paper describes dynamical quantum effects of nontrivial topology and shows that they can be revealed by studying parametric resonance in closed spin-1/2 chains. The topology manifests in the response to turning on parametric modulation. For a rapid turn-on, it leads to zeroing of time-averaged spatial correlations of the longitudinal magnetization and its independence of the modulation frequency. For a slow turn-on, the dependencies of the spin parameters on the modulation parameters are different, but also qualitatively distinct from conventional behavior. Moreover, they display hysteresis. In the thermodynamic limit, the derivatives of the time-averaged spatial correlators and the magnetization are discontinuous at the transition to the topological regime. The transition is controlled just by the modulation frequency, which facilitates its exploration in the experiment. An appropriate platform is multi-qubit simulators of spin chains, cf. [18, 20]. Related nontrivial dynamical effects should be expected also in the spin chains that are actively studied in various condensed-matter systems [34]; their analysis requires extending the theory to allow for a more general spin coupling.

ACKNOWLEDGMENTS

We acknowledges partial support from the U.S. Defense Advanced Research Projects Agency (Grant No. HR0011-23-2-004) and from the Gordon and Betty Moore Foundation Award No. GBMF12214.

Supplemental Material

SM: I. MAPPING TO THE KITAEV CHAIN

We consider a chain of N spins in a strong magnetic field with nearest-neighbor XY coupling. The coupling along the x-axis is sinusoidally modulated at frequency ω_F close to twice the spin Larmor frequency. Equivalently, the formulation applies to a qubit chain, with ω_0 being the transition frequency. We assume that the chain is closed, so that the site N+1 coincides with the site 1. The Hamiltonian of the chain is

$$\hat{H}_{lab} = -\frac{1}{2}\omega_0 \sum_{n=1}^{N} \sigma_n^z - J_{xx}(t) \sum_{n=1}^{N} \sigma_n^x \sigma_{n+1}^x - J_{yy} \sum_{n=1}^{N} \sigma_n^y \sigma_{n+1}^y,$$

$$J_{xx}(t) = J_{xx} + 2F\cos(\omega_F t), \qquad (\hbar = 1),$$
(S1)

where $\sigma_n^{x,y,z}$ are the Pauli matrices for an nth spin, ω_0 is the Larmor (transition) frequency, J_{xx} and J_{yy} are the coupling parameters, and F and ω_F are the modulation amplitude and frequency, respectively, $|\omega_F - 2\omega_0| \ll \omega_F$. We consider the regime of weak coupling in the sense that $|J_{xx}|$, $|J_{yy}|$, and |F| are much smaller than ω_0 . The values of F and ω_F can depend on time, generally, but they remain nearly constant on the time scale ω_F^{-1} , that is $|(dF/dt)|, |d\omega_F/dt| \ll \omega_F^2$.

In contrast to the conventional problem of parametric resonance, where magnons are bosonic excitations and it is necessary to take into account their interaction to prevent the runaway, i.e., to take into account the nonlinearity [1], in the case of the spin chain the nonlinearity is already "built in". It is convenient to analyze resonant parametric modulation by going to the rotating frame at frequency $\omega_F/2 \approx \omega_0$ using the transformation

$$\hat{U}(t) = \exp\left\{\frac{1}{4}i\int^t dt'\omega_F(t')\sum_{n=1}^N \sigma_n^z\right\}.$$
 (S2)

In the rotating wave approximation (RWA), the transformed Hamiltonian of the system $U^{\dagger}H_{\text{lab}}U - iU^{\dagger}\dot{U}$ has the form

$$\hat{H}_{\text{RWA}} = \frac{1}{2} \mu \sum_{n=1}^{N} \sigma_n^z - J \sum_{n=1}^{N} (\sigma_n^+ \sigma_{n+1}^- + \sigma_{n+1}^+ \sigma_n^-) - F \sum_{n=1}^{N} (\sigma_n^+ \sigma_{n+1}^+ + \sigma_{n+1}^- \sigma_n^-),$$

$$\mu = \frac{1}{2} \omega_F - \omega_0, \qquad J = J_{xx} + J_{yy}, \qquad \sigma_m^{\pm} = \frac{1}{2} (\sigma_n^x \pm i \sigma_n^y). \tag{S3}$$

The Hamiltonian \hat{H}_{RWA} clearly shows that resonant parametric excitation leads to birth or annihilation of pairs of magnons or, equivalently, to upward or downward flips of qubits in pairs.

Next, we apply the standard Jordan-Wigner transformation

$$\sigma_n^z = 1 - 2a_n^{\dagger} a_n, \qquad \sigma_n^+ = \left[\prod_{m=1}^{n-1} (2a_m^{\dagger} a_m - 1) \right] a_n, \qquad a_n = \left[\prod_{m=1}^{n-1} (-\sigma_m^z) \right] \sigma_n^+, \qquad n = 1, \dots, N$$
 (S4)

where a_n^{\dagger} and a_n are fermionic creation and annihilation operators, respectively, which satisfy $\{a_n, a_m\}_+ = \{a_n^{\dagger}, a_m^{\dagger}\}_+ = 0$ and $\{a_n, a_m^{\dagger}\}_+ = \delta_{n,m}$. cf. [12].

When changing to the fermionic operators in a chain of period N, care must be taken of the terms $\sigma_N^{\alpha}\sigma_{N+1}^{\beta} \equiv \sigma_N^{\alpha}\sigma_1^{\beta}$ in the Hamiltonian (S3) with $\alpha, \beta = \pm$. These terms simplify since the original Hamiltonian and the RWA Hamiltonian preserve the parity of states, $P^{\dagger}\hat{H}_{\text{lab}}P = \hat{H}_{\text{lab}}$ and $P^{\dagger}\hat{H}_{\text{RWA}}P = \hat{H}_{\text{RWA}}$, where $P = \exp[i(\pi/2)\sum_{n=1}^{N}\sigma_n^z]$. This is a consequence of spins flipped in pairs in resonant parametric excitation and, respectively, of the fermionic excitations being created or annihilated in pairs. We assume that in the initial state $|\Psi_0\rangle$, i.e., in the state before the modulation is turned on, all spins are polarized along the magnetic field or, equivalently, all qubits are in the ground state, $|\Psi_0\rangle = |\uparrow_1 \dots \uparrow_N\rangle$. This state has even parity. For even N this leads to the boundary condition $a_{N+1} = -a_1$. We then change to the fermionic operators c_k, c_k^{\dagger} using the Fourier transform

$$a_n = N^{-1/2} e^{-i\pi/4} \sum_k c_k e^{ikn}, \qquad k = \pi \frac{2m-1}{N} \qquad \left(m = -(N/2) + 1, -(N/2) + 2, ..., N/2\right),$$
 (S5)

and write the RWA-Hamiltonian of the parametrically modulated chain in the form

$$\hat{H} = -\frac{1}{2} \sum_{k} \vec{c}_{k}^{\dagger} \left(M_{k} \tau^{z} + F_{k} \tau^{x} \right) \vec{c}_{k}, \quad M_{k} = \mu - 2J \cos k, \quad F_{k} = 2F \sin k.$$
 (S6)

Here $\vec{c}_k = \begin{pmatrix} c_k \\ c_{-k}^{\dagger} \end{pmatrix}$ are the Nambu vectors and $\tau^{x,y,z}$ are Pauli-matrices.

It follows from the known results on the Kitaev chain [13] that the range of relatively large detuning of the parametric drive from resonance, $|\mu/2J| \equiv |(\omega_F - 2\omega_0)/4J| > 1$, is topologically trivial. The range $|\mu/2J| \equiv |(\omega_F - 2\omega_0)/4J| < 1$ is topologically nontrivial. We emphasize that we are considering a closed chain, there are no Majorana fermions at the chain edges. We are looking for the manifestation of topological features in the response to changing the modulation parameters.

In terms of the eigenstates $|n_k\rangle$ of the fermions described by the operators c_k , the initially occupied state is

$$|\Psi_0\rangle = \prod_k |0_k\rangle, \qquad c_k |0_k\rangle = 0.$$

While $|\Psi_0\rangle$ is an eigenstate of the Hamiltonian \hat{H} in (S6) for F=0, it is not the ground state for |F|>0. This is not surprising, since the actual states of our periodically driven system are Floquet states and there is no reason for the system to go to the state where \hat{H} is minimal.

The Hamiltonian (S6) can be diagonalized by the transformation $U(k) = \exp[-i(\theta_k/2)\tau^y]$, which relates c_k, c_k^{\dagger} to new fermionic operators d_k, d_k^{\dagger} ,

$$d_k = c_k \cos \theta_k / 2 + c_{-k}^{\dagger} \sin \theta_k / 2, \quad d_{-k}^{\dagger} = -c_k \sin \theta_k / 2 + c_{-k}^{\dagger} \cos \theta_k / 2, \quad \tan \theta_k = \frac{F_k}{M_k}.$$
 (S7)

In terms of these operators

$$\hat{H} \to \hat{H}_0 = \frac{1}{2} \sum_k \varepsilon_k [-\operatorname{sgn}(M_k \cos \theta_k)] \vec{d}_k^{\dagger} \tau^z \vec{d}_k, \quad \varepsilon_k = \sqrt{M_k^2 + F_k^2}.$$
 (S8)

A standard convention is that quasiparticles excited by the operators $\{d_k^{\dagger}\}$ have positive energies $\varepsilon_k/2$. This corresponds to the values θ_k such that $M_k \cos \theta_k < 0$. As k changes, function θ_k changes as well. However, the sign of $M_k \cos \theta_k < 0$ does not. As seen from Eq.(S7), $\theta_{-k} = -\theta_k$.

We are interested in evaluating time-averaged correlation functions of the parametrically modulated spin/qubit chain. The averaging is done over time T that exceeds the reciprocal gap $T \gg \max_k \varepsilon_k^{-1}$. In the topologically trivial regime the gap $\min_k \varepsilon_k$ is nonzero for all F and the averaging is well-defined. The correction that emerges in the nontrivial regime is discussed in the main text.

SM: II. ANALYTICAL RESULTS FOR SUDDEN QUENCH

A. Time-averaged correlations of fermions

We start with the dynamics where the drive amplitude is sharply turned on at time t=0 from F=0 to a final value F. The change of F is slow on the time scale ω_F^{-1} , but fast on the time scale ε_k^{-1} . After the modulation has been turned on, the operators d_k evolve in time as $d_k(t) = \exp(-i\varepsilon_k t)d_k(+0)$, where we use t=+0 to indicate that this is the instant of time at which the field has been just turned on. The rotation angle θ_k is independent of time, $\theta_k(t) = \theta_k(+0)$. From Eq. (S7)

$$c_k^{\dagger}(t)c_k(t) = d_k^{\dagger}d_k\cos^2\theta_k/2 + d_{-k}d_{-k}^{\dagger}\sin^2\theta_k/2 - \frac{1}{2}\left(d_k^{\dagger}d_{-k}^{\dagger}e^{2i\varepsilon_kt} + d_{-k}d_ke^{-2i\varepsilon_kt}\right)\sin\theta_k,$$

where $d_k = d_k(+0)$. Only the terms proportional to $d_k^{\dagger} d_k$ and $d_{-k} d_{-k}^{\dagger}$ contribute to the time-averaged terms in this expression,

$$\begin{split} \overline{c_k^{\dagger}(t)c_k(t)} &= d_k^{\dagger} d_k \cos^2 \theta_k / 2 + d_{-k} d_{-k}^{\dagger} \sin^2 \theta_k / 2 \\ &= (\cos^4 \theta_k / 2 + \sin^4 \theta_k / 2) c_k^{\dagger} c_k + \frac{1}{4} \sin 2\theta_k (c_k^{\dagger} c_{-k}^{\dagger} + c_{-k} c_k) + \frac{1}{2} \sin^2 \theta_k c_{-k} c_{-k}^{\dagger}, \end{split}$$

where the overline indicates time-averaging and $c_k = c_k(+0)$, $c_k^{\dagger} = c_k^{\dagger}(+0)$.

For the sudden turn-on of the modulation, the expectation value of this average has to be taken on the state $|\Psi_0\rangle$, which is the state of the system before the turn-on. It corresponds to the vacuum of the c_k fermions, and we can disregard its change over the infinitesimal (on the scale $\max \varepsilon_k^{-1}$) time it takes to turn on the modulation. Then only the term proportional to $c_{-k}(0)c_{-k}^{\dagger}(0)$ contributes to $\overline{c_k^{\dagger}(t)c_k(t)}$, so that

$$\langle c_k^{\dagger}(t)c_k(t)\rangle = \frac{1}{2}\sin^2\theta_k,$$
 (S9)

where, as in the main text, $\langle \cdot \rangle$ denotes the time-averaged expectation value.

Similarly, we have

$$\overline{c_k^{\dagger}(t)c_{-k}^{\dagger}(t)} = -\frac{1}{2}\sin\theta_k \left[d_k(+0)d_k^{\dagger}(+0) - d_{-k}^{\dagger}(+0)d_{-k}(+0) \right].$$

which gives for the expectation value

$$\langle c_k^{\dagger}(t)c_{-k}^{\dagger}(t)\rangle = -\frac{1}{4}\sin 2\theta_k. \tag{S10}$$

We emphasize that, in Eqs. (S9) and (S10), the value of θ_k refers to the modulation having been turned on, $\theta_k \equiv \theta_k(+0)$. It is given by Eq. (S7).

B. Magnetization and spatial correlations in the spin chain

The results on the correlators of the c_k operators allow one to time-averaged parameters of the spin chain using Eqs. (S4) and (S5). For the change of the scaled magnetization due to parametric excitation we have from Eqs. (S7) and (S9) in the thermodynamic limit $N \to \infty$

$$1 - \langle \sigma_n^z \rangle = \frac{2}{N} \sum_k \langle c_k^{\dagger} c_k \rangle = \frac{1}{2\pi} \int_{-\pi}^{\pi} \sin^2 \theta_k dk = \frac{1}{2\pi} \int_{-\pi}^{\pi} \left(\frac{F_k}{\varepsilon_k} \right)^2 dk$$
$$= -\frac{F}{\pi} \text{Im} \int_{-\pi}^{\pi} \frac{2 \sin k}{\mu - 2J \cos k + 2iF \sin k} dk$$

Changing to integration over $w = \exp(ik)$, we obtain

$$1 - \langle \sigma_n^z \rangle = \frac{F}{2\pi} \text{Im} \oint \frac{dw}{w} \frac{w^2 - 1}{P_1(w)}, \qquad P_1(w) = (F - J)w^2 + \mu w - (F + J), \tag{S11}$$

The contour integral is taken over the unit circle in the complex w-plane. The integrand has a pole at w = 0 and two poles $w_{\pm}^{(1)}$ given by the zeros of $P_1(w)$,

$$w_{\pm}^{(1)} = \frac{-\mu \pm \sqrt{\mu^2 - 4(J^2 - F^2)}}{2(F - J)}.$$
 (S12)

In the topological regime, both $w_{\pm}^{(1)}$ lie inside (outside) the unit circle for FJ < 0 (FJ > 0). In the trivial regime, for $\mu > 0$ ($\mu < 0$) the root $w_{\pm}^{(1)}$ ($w_{\pm}^{(1)}$) lies inside the unit circle, whereas the other root lies outside. Then, from Eq. (S11),

$$1 - \langle \sigma_n^z \rangle = \left\{ \begin{array}{l} [F^2/(F^2 - J^2)] \left\{ 1 - |\mu| \left[\mu^2 + 4(F^2 - J^2) \right]^{-1/2} \right\}, & |\mu| > 2|J| \\ (1 + |J/F|)^{-1}, & |\mu| < 2|J|. \end{array} \right.$$
 (S13)

1. The pair correlator

A quantity of significant interest and importance is the spin correlator

$$Q^{z}(m) = \langle \Delta \sigma_{n}^{z} \Delta \sigma_{n+m}^{z} \rangle = \frac{4}{N^{2}} \sum_{k_{1}, \dots, k_{4}} \langle c_{k_{1}}^{\dagger} c_{k_{2}} c_{k_{3}}^{\dagger} c_{k_{4}} \rangle e^{i(k_{1} - k_{2})m} \delta_{k_{1} - k_{2}, k_{4} - k_{3}},$$

$$\Delta \sigma_{n}^{z} = \sigma_{n}^{z} - \langle \sigma_{n}^{z} \rangle, \tag{S14}$$

where $k_1 \neq k_2$ and $k_3 \neq k_4$. There are two different ways of pairing the values of k_i :

$$k_1 = k_4 \& k_2 = k_3 \text{ or } k_1 = -k_3 \& k_2 = -k_4.$$

Applying the parings gives, in the thermodynamic limit,

$$Q^{z}(m) = \frac{4}{N^{2}} \sum_{k,q} \left[\langle c_{k}^{\dagger} c_{k} \rangle \langle c_{q} c_{q}^{\dagger} \rangle - \langle c_{k}^{\dagger} c_{-k}^{\dagger} \rangle \langle c_{q} c_{-q} \rangle \right] e^{i(k-q)m} = -\left| Q_{1}(m) \right|^{2} + \left| Q_{2}(m) \right|^{2}$$

$$Q_{1}(m) = \frac{2}{N} \sum_{k} \langle c_{k}^{\dagger} c_{k} \rangle e^{ikm} = \frac{1}{N} \sum_{k} \sin^{2} \theta_{k} \cos(mk),$$

$$Q_{2}(m) = \frac{-2i}{N} \sum_{k} \langle c_{k}^{\dagger} c_{-k}^{\dagger} \rangle e^{ikm} = \frac{-1}{2N} \sum_{k} \sin 2\theta_{k} \sin(mk),$$
(S15)

where we used the results from equations (S9) and (S10). To calculate $Q_{1,2}(m)$, we change from the sums to integrals over k and then from integration over k to integration over the unit circle |w| = 1. We choose $w = e^{ik}$ where the integrand contains $\exp(imk)$ and $w = e^{-ik}$ when the integrand contains $\exp(-imk)$; in the latter case the direction of going around the contour |w| = 1 is changed to the opposite. After simple algebra, we obtain

$$Q_{\alpha}(m) = \frac{F}{4\pi} \operatorname{Im} \oint dw \, w^{|m|-1} (w^2 - 1) [P_1^{-1}(w) - (-1)^{\alpha} P_2^{-1}(w)],$$

$$P_{\alpha}(w) = F(w^2 - 1) - (-1)^{\alpha} [\mu w - J(w^2 + 1)] \quad (\alpha = 1, 2).$$
(S16)

In the topological regime, where $|\mu/2J| < 1$, the polynomials $P_1(w)$ and $P_2(w)$ have no roots with |w| < 1 for FJ > 0 and FJ < 0, respectively. Therefore, from Eq. (S16), $Q_1(m) = -Q_2(m)$ for FJ > 0 and $Q_1(m) = Q_2(m)$ for FJ < 0. Thus, we see from Eq. (S15) that the time-averaged pair correlation function of the z-components of the spins is zero for all values of m for $|\mu/2J| < 1$. This is an unexpected and nontrivial feature noted in the main text.

In the trivial regime, where $|\mu/2J| > 1$, both $P_1(w)$ and $P_2(w)$ have one root with |w| < 1, and then $Q^z(m)$ is nonzero. For instance, for the nearest-neighbor correlator, m = 1, taking into account the contributions from the poles that are inside the unit circle, we obtain

$$Q^{z}(1) = \frac{2F^{2}(\mu^{2} - 4J^{2})}{r_{\mu}^{2}(\mu^{2} - 2J^{2} + 2F^{2} + |\mu|r_{\mu})}, \quad |\mu/2J| > 1,$$
(S17)

where $r_{\mu} \equiv \sqrt{\mu^2 - 4J^2 + 4F^2}$. We see that $Q^z(1)$ is continuous at $|\mu| \to 2|J|$, but its derivative over μ is discontinuous. The function $Q^z(1)$ first increases with the increasing $|\mu|$ beyond the critical value $|\mu| = 2|J|$, but then it falls off as μ^{-2} for large $|\mu|$.

2. The three-site correlator

Calculating the three-site correlator $\langle \Delta \sigma_{n_1}^z \Delta \sigma_{n_2}^z \Delta \sigma_{n_3}^z \rangle$ comes to integrating the expectation value of the time-averaged product $c_{k_1}^{\dagger} c_{k_2} c_{k_3}^{\dagger} c_{k_4} c_{k_5}^{\dagger} c_{k_6}$ with the weight $\prod_j \exp[-i n_j (k_j - k_{j+1})]$. In turn, this comes to calculating 8 combinations where we take k_i so that the fermionic operators are paired into products with the total momentum transfer equal to zero, i.e., $c_{k_i}^{\dagger} c_{k_i}$, $c_{k_i}^{\dagger} c_{-k_i}^{\dagger}$, and $c_{k_i} c_{-k_i}$. This allows us to express the three-site correlator in terms of the functions $\mathcal{Q}_{1,2}(m)$ given by Eq. (S16),

$$\langle \Delta \sigma_n^z \Delta \sigma_{n+m}^z \Delta \sigma_{n+l}^z \rangle = 2Q_1(m)Q_1(l)Q_1(m-l) - 2Q_1(m)Q_2(l)Q_2(l-m) + 2Q_1(l)Q_2(m)Q_2(l-m) - 2Q_1(m-l)Q_2(m)Q_2(l),$$
(S18)

where l > m > 0.

As discussed above, $Q_1(m) = -\operatorname{sgn}(FJ)Q_2(m)$ in the topological regime. Therefore, it is seen from Eq. (S18) that the three-site correlator is equal to zero in the topological regime. Higher order correlators can be shown to also vanish in the topological regime.

C. The correlator of the transverse spin components

Another correlator discussed in the main text is that of the transverse spin components $\langle \sigma_n^+ \sigma_{n+1}^- \rangle = -\langle c_{n+1}^\dagger c_n \rangle = -Q_1(1)/2$. This gives

$$\langle \sigma_n^+ \sigma_{n+1}^- \rangle = \begin{cases} -\operatorname{sgn}(\mu) J F^2 (|\mu| - r_\mu)^2 / [4r_\mu (J^2 - F^2)^2], & |\mu| > 2|J| \\ -\operatorname{sgn}(FJ) (\mu/4F) (1 + |J/F|)^{-2}, & |\mu| < 2|J|. \end{cases}$$
(S19)

In the main text, we plot the absolute value of $\langle \sigma_n^+ \sigma_{n+1}^- \rangle$. Given that $\langle \sigma_n^+ \sigma_{n+1}^- \rangle$ is real and negative for $\mu J > 0$, we plot the expressions (S19) taken with the opposite sign.

D. Relation to the winding number

As discussed in the main text, the winding number for the Kitaev chain is defined as $\nu = (2\pi)^{-1} \int_{-\pi}^{\pi} dk (d\theta_k/dk)$, where θ_k is defined in equation (S7). From this equation,

$$\nu = \frac{1}{2\pi} \int_{-\pi}^{\pi} dk \left(\frac{M_k (dF_k/dk) - F_k (dM_k/dk)}{\varepsilon_k^2} \right) = \frac{1}{\pi} \int_{-\pi}^{\pi} dk \left(\frac{F \cos kM_k - J \sin kF_k}{\varepsilon_k^2} \right)$$

$$= \frac{1}{\pi} \operatorname{Im} \left\{ \int_{-\pi}^{\pi} dk \frac{iF \cos k + J \sin k}{\mu - 2J \cos k + 2iF \sin k} \right\}$$
(S20)

As before, we can change to integration over $w = e^{ik}$, which gives

$$\nu = \frac{1}{2\pi} \text{Im} \oint \frac{dw}{w} \frac{(F-J)w^2 + (F+J)}{P_1(w)},$$
 (S21)

where $P_1(w)$ is defined in Eq. (S11). We can also write ν in the same form, but with $F \to -F$ in the numerator and $P_1(w) \to P_2(w)$. Clearly, the value of the winding number is determined by the structure of the poles of $P_1(w)$ and $P_2(w)$, which also determine the structure of the time-averaged spin observables we discussed above. To further see this, we assume FJ > 0. Then, we can write ν as

$$\nu = \frac{1}{2\pi} \text{Im} \left\{ (F - J) \oint dw \frac{w}{P_1(w)} + (F + J) \oint \frac{dw}{w} \frac{1}{P_1(w)} \right\}.$$
 (S22)

In the topological regime, the poles of $P_1(w)$ lie outside the unit circle, and therefore $\nu=(F+J)/P_1(0)=-1$. For FJ<0, writing the integral in terms of P_2 and taking into account that P_2 does not have poles with |w|<1 in the topological regime, we obtain $\nu=(J-F)/P_2(0)=1$. A calculation for $|\mu/2J|>1$ shows that $\nu=0$ in this range. This is fully analogous to the calculations of the magnetization and the spin correlators above, revealing explicitly the relation of these calculations to the winding number.

SM: III. ANALYTICAL RESULTS FOR ADIABATIC SWITCHING

A. Adiabatic evolution

In this section, we consider the dynamics where the drive amplitude is slowly switched on, varying monotonously from F(t=0)=0 to $F(t_f)=F_f\equiv F$ (to maintain consistence with the notations in the previous section we use F for the finite value of the drive amplitude). Expectation values of the spin operators are then time-averaged from $t>t_f$ till $t=t_f+T$.

The Heisenberg equations for the operators d_k are

$$\dot{\vec{d}}_k = -i[\vec{d}_k, H_0] - U^{\dagger}(k)\dot{U}(k)\vec{d}_k, \quad \vec{d}_k = \begin{pmatrix} d_k \\ d_{-k}^{\dagger} \end{pmatrix}, \quad U(k) = \exp\left[-i\frac{\theta_k(t)}{2}\tau^y\right],$$

where we take into account that the rotation angle $\theta_k(t) = \text{Arctan}[F_k(t)/M_k]$ depends on time, since $F_k(t) = 2F(t)\sin k$ varies in time; we remind that we define θ_k as a continuous function of k. Therefore, in the topological regime, $\operatorname{sgn} \theta_k$

does not change where M_k goes through zero; also, $\operatorname{sgn} \theta_k(t)$ does not change when $F_k(t)$ is a monotonous function of time.

For $M_k \cos \theta_k > 0$ the above equations take the form

$$\dot{d}_k = i\varepsilon_k d_k + \frac{1}{2}\dot{\theta}_k d_{-k}^{\dagger}, \quad \dot{d}_{-k}^{\dagger} = -i\varepsilon_k d_{-k}^{\dagger} - \frac{1}{2}\dot{\theta}_k d_k. \tag{S23}$$

where $\varepsilon_k \equiv \varepsilon_k(t) = \sqrt{M_k^2 + F_k(t)^2}$.

The adiabatic approximation refers to the case where $|\dot{\theta}_k| \ll \varepsilon_k$. In this approximation,

$$d_k(t) = d_k(0) \exp\left[i \int_0^t dt' \varepsilon_k(t')\right] \quad (M_k \cos \theta_k > 0).$$

The value of $d_k(0)$ here is found from Eq. (S7) by noting that $\theta_k(0)$ equals either 0 or π for $M_k \neq 0$. In the considered case $M_k \cos \theta_k > 0$, we have $d_k(0) = c_k(0)$ for $M_k > 0$ and $d_k(0) = c_{-k}^{\dagger}(0)$ for $M_k < 0$. Then from equation $\vec{c}_k = U(k)\vec{d}_k$

$$c_k(t) = \begin{cases} c_k(0)e^{i\Phi(t)}\cos[\theta_k(t)/2] - c_{-k}^{\dagger}(0)e^{-i\Phi(t)}\sin[\theta_k(t)/2], & M_k > 0 \ [\theta_k(0) = 0] \\ c_{-k}^{\dagger}(0)e^{i\Phi(t)}\cos[\theta_k(t)/2] - c_k(0)e^{-i\Phi(t)}\sin[\theta_k(t)/2], & M_k < 0 \ [\theta_k(0) = \pi] \end{cases}$$
(S24)

where $\Phi(t) = \int_0^t dt' \varepsilon_k(t')$. Thus, the fermionic expectation values are given by

$$\langle c_k^{\dagger}(t)c_k(t)\rangle = \frac{1}{2}(1 - |\cos\theta_k|) = \frac{\varepsilon_k - |M_k|}{2\varepsilon_k},$$

$$\langle c_k^{\dagger}(t)c_{-k}^{\dagger}(t)\rangle = \frac{-1}{2}\sin\theta_k = -\frac{F_k}{2\varepsilon_k}\operatorname{sgn} M_k.$$
(S25)

The last terms in the right-hand sides of Eq. (S25) apply also for $M_k \cos \theta_k < 0$. Equations (S25) allow us to calculate the correlators $Q_{1,2}(m)$, Eq. (S15), which determine the time-averaged expectation values and the correlation functions of the spins,

$$Q_1(m) = \frac{2}{N} \sum_k \langle c_k^{\dagger} c_k \rangle e^{ikm} = \delta_{m,0} - \frac{1}{N} \sum_k \sqrt{\frac{M_k^2}{M_k^2 + F_k^2}} \cos(mk),$$

$$Q_2(m) = \frac{-2i}{N} \sum_k \langle c_k^{\dagger} c_{-k}^{\dagger} \rangle e^{ikm} = \frac{-1}{N} \sum_k \sin \theta_k \sin(mk).$$
(S26)

One can change from summation to integration over k in these expressions, and then to integration over $w = \exp(ik)$ or $w = \exp(-ik)$. The resulting integrals have branching points inside the unit circle |w| = 1 for $P_1(w)P_2(w) = 0$, where the polynomials $P_{1,2}(w)$ are defined in Eq. (S16). Therefore the structure of the integrals is different in the topologically trivial and topologically nontrivial regimes. This leads to a different dependence of the spin correlators on $\mu = \frac{1}{2}\omega_F - \omega_0$, and thus on the parametric drive frequency ω_F . However, the explicit integration is cumbersome. In the main text we show the results obtained by calculating the integrals numerically.

B. Scaling of nonadiabatic corrections

The adiabaticity condition $|\dot{\theta}_k| \ll \varepsilon_k$ breaks down where the energy gap is small. Inside the topological regime, $|\mu/2J| < 1$, the gap closes for F(t=0) = 0 and $k = \pm k_{\mu}$, where

$$k_{\mu} = \arccos(\mu/2J).$$

Therefore, the adiabatic approximation does not apply for small |F| and $|k| - k_{\mu}|$. The explicit applicability condition follows from Eq. (S7) for θ_k , which shows that

$$\dot{\theta}_k = 2\dot{F}\sin k \, M_k / \varepsilon_k^2.$$

The "nonadiabatic" region of k, where $\varepsilon_k \lesssim |\dot{\theta}_k|$, is limited to $|k| - k_\mu| \lesssim |\dot{F}/G_\mu|^{1/2}$, where $G_\mu = J(4J^2 - \mu^2)^{1/2}$. The resulting corrections to the spin correlators and to $\langle \sigma_z \rangle$ are proportional to the size of this region. As described in the main text, they scale as $|\dot{F}/G_\mu|^{1/2}$. We note that such adiabaticity breaking occurs only for small |F(t)|; for $|F(t)/J| \gtrsim |\dot{F}/G_\mu|^{1/2}$ the adiabaticity is restored.

The energy gap closes also at the boundary of the topological regime, for $\mu/2J = 1$ and k = 0, and for $\mu/2J = -1$ and $k = \pi$. For $|\mu/2J| = 1$, the range of k where the adiabaticity is broken scales as $|\dot{F}/J^2|^{1/3}$ for $|F(t)/J| < |\dot{F}/J^2|^{1/3}$. We note that the dynamical equations can be solved in the explicit form where the gap is closed, i.e., $M_k = 0$. In this case, from the Heisenberg equations for the fermionic operators $c_k(t)$ we find

$$c_k(t) = \cos\left(\int_0^t F_k(t')dt'\right)c_k(0) + i\sin\left(\int_0^t F_k(t')dt'\right)c_{-k}^{\dagger}(0).$$
 (S27)

The time evolution of $c_k(t)$ as described by Eq. (S27) is reminiscent of Rabi oscillations. Oscillations of $c_k(t)$ persist away from the points $\varepsilon_k = 0$. In the adiabatic regime they have frequency $\varepsilon_k(t)$ and are superposed on the smooth adiabatic evolution; they lead to oscillations of the spin variables. Of primary interest for the experiment are time-averaged spin correlators that we calculate. The simulation results shown in the main text also refer to time-averaged spin correlators, as we discuss in Sec. SM: V.

C. Hysteresis

The difference between the topological and trivial regimes leads to a memory effect. Consider a state with a given drive amplitude F_f and the scaled detuning of the drive frequency μ_f in the topological regime $|\mu_f/2J| < 1$. The system can be brought to this state in two different ways. First, one can slowly switch on the drive amplitude at $\mu = \mu_f$. The resulting average pair correlators of the fermions are given by Eq. (S25). Alternatively, one can adiabatically switch on the drive amplitude at a detuning $\mu = \mu_0$ that lies in the trivial regime, $|\mu_0/2J| > 1$, and then slowly change μ to μ_f . Since the initial value of $\operatorname{sgn} M_k = \operatorname{sgn} \mu_0$ is the same for all k and the sign of $M_k \cos \theta_k$ is not changing with the slowly varying μ , the resulting expectation values of the correlators in the topological regime become

$$\langle c_k^{\dagger}(t)c_k(t)\rangle = \frac{\varepsilon_k - M_k \operatorname{sgn} \mu_0}{2\varepsilon_k},$$

$$\langle c_k^{\dagger}(t)c_{-k}^{\dagger}(t)\rangle = -\frac{F_k}{2\varepsilon_k} \operatorname{sgn} \mu_0$$
(S28)

(we assume here that k is away from the critical value 0 or π , depending on sgn μ_0)

As shown in the main text, this leads to a pronounced difference in the values of the spin correlators for the same drive amplitude and detuning depending on how these parameters have been reached, and thus to a memory effect. This effect can be observed using the observable $\langle \sigma_n^+ \sigma_{n+1}^- \rangle$ shown in the main text as well as other observables, such as $1 - \langle \sigma_z \rangle$ and $\mathcal{Q}^z(1)$. We present the results for the latter observables in Fig. S1. We note that, when the scaled detuning of the drive frequency μ is changed along the second path, i.e., starting with $|\mu(0)/2J| > 1$, the phase transition at $|\mu(t)/2J| = 1$ is crossed, leading to generation of excitations near k = 0 or π via the Kibble-Zurek mechanism [29, 30]. The resulting corrections to the time-averaged expectation values of the spin correlators and $\langle \sigma_z \rangle$ remain small in the thermodynamic limit for a slowly varying μ .

SM: IV. SOLVING THE SCHRÖDINGER EQUATION FOR A SLOWLY TURNED ON DRIVE

The Hamiltonian (S6) couples fermions of opposite momenta. Thus, the wave function of the system can be written as

$$|\Psi(t)\rangle = \prod_{k>0} \left[\sum_{m,n} A_{mn}(k,t) | m_{-k}, n_k \rangle \right],$$

where $m_k, n_k = \{0, 1\}$ are the occupation numbers of the states of c_k -fermions, $c_k | n_k \rangle = n_k | n_k - 1 \rangle$. The Schrödinger equation for the system is reduced to a set of equations for $A_{mn}(k)$ for each k. Moreover, the equations for even and odd m + n are uncoupled.

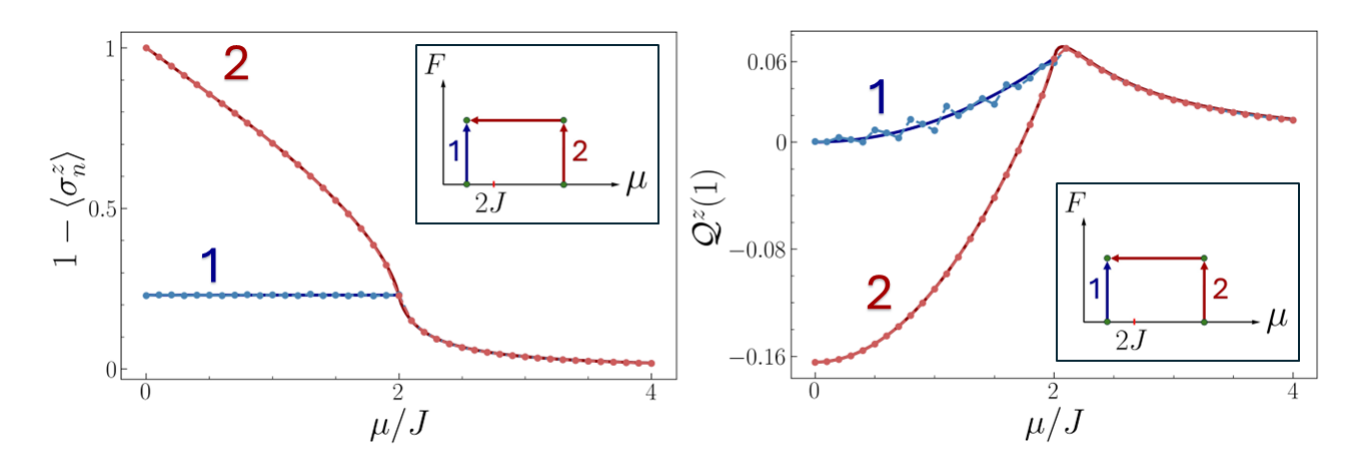


FIG. S1. The time-averaged correlators $1 - \langle \sigma_z \rangle$ (left panel) and $\mathcal{Q}^z(1)$ (right panel) obtained by slowly increasing the drive to $F_f/J = 0.5$ for a fixed μ (line 1 and blue dots) and by slowly turning on the drive to the same F_f/J in the trivial regime and then slowly changing the modulation frequency to arrive at the same μ (line 2 and red dots). The simulations refer to N = 40 and $F(t) = F_f t/\tau_{\rm sl}$ with $\tau_{\rm sl} = 10^3/J$.

The initial condition $|\Psi(0)\rangle = |\Psi_0\rangle$ gives $A_{mn}(k,0) = \delta_{m,0}\delta_{n,0}$, $\forall k$. Therefore of interest are the equations that couple $A_{00}(k,t)$ and $A_{11}(k,t)$. In the Hamiltonian form, they read

$$i\dot{A}_{ii}(k,t) = \partial H_k / \partial A_{ii}^*(k,t) \quad (i=0,1),$$

$$H_k = M_k \left[|A_{00}(k,t)|^2 - |A_{11}(k,t)|^2 \right] - F_k \left[A_{00}(k,t) A_{11}^*(k,t) + \text{c.c.} \right],$$

$$A_{00}(k,0) = 1, \quad A_{11}(k,0) = 0,$$
(S29)

or, in the explicit form,

$$i\dot{A}_{00} = M_k A_{00} - F_k A_{11}, \quad i\dot{A}_{11} = -M_k A_{11} - F_k A_{00} \quad [A_{ii} \equiv A_{ii}(k,t)],$$

whereas $A_{01}(k,t) = A_{10}(k,t) = 0$. We note that the functions A_{00} , A_{11} describe also the time evolution of the fermionic operators in the Heisenberg picture, with $c_{-k}^{\dagger}(t) = A_{00}(k,t)c_{-k}^{\dagger}(0) + A_{11}^{*}(-k,t)c_{k}(0)$. Such correspondence simplifies a comparison with the previous sections. However, in this section it is more natural to consider functions, rather than operators, and therefore we are using the Schrödinger picture.

A. The WKB approximation

Equations (S29) for $A_{00} \equiv A_{00}(k,t), A_{11} \equiv A_{11}(k,t)$ can be written as

$$\ddot{A}_{00} = \frac{-i\dot{F}_k}{F_k} \left(i\dot{A}_{00} - M_k A_{00} \right) - \varepsilon_k^2 A_{00} - i\dot{M}_k A_{00}, \qquad A_{11} = -(i\dot{A}_{00} - M_k A_{00}) / F_k(t)$$
 (S30)

We will seek the solution of these equations in the WKB approximation. This approximation relies on the slowness of the variation of F_k and M_k . The small parameter of the theory is $|\dot{\varepsilon}_k|/\varepsilon_k^2$. For simplicity, we present the results for the case of time-independent M_k , although they immediately extend to a slowly varying in time M_k .

The structure of Eq. (S30) for A_{00} is different from the more conventional structure of the equations solved in the WKB approximation, where there are no terms with first derivatives. These terms can be eliminated (see below), but it is more convenient to seek the solution as a sum of an eikonal and non-eikonal terms. To the first order in $|\dot{\varepsilon}_k|/\varepsilon_k^2 \ll 1$ the eikonal term is

$$A_{00}(k,t) = A_{1}(k,t) + A_{2}(k,t); \quad A_{1}(k,t) = C_{k1} \exp[iS(t)], \quad S(t) \approx S^{(0)}(t) + S^{(1)}(t),$$

$$S^{(0)}(t) = -\int_{0}^{t} \varepsilon_{k}(t')dt' (\operatorname{sgn} M_{k}), \qquad S^{(1)}(t) = \frac{i}{2} \left(\log \frac{\varepsilon_{k}(t)}{\varepsilon_{k}(0)} - \log \frac{\varepsilon_{k}(t) + |M_{k}|}{\varepsilon_{k}(0) + |M_{k}|} \right), \tag{S31}$$

where C_{k1} is a constant to be determined by the initial conditions. The WKB approximation implies that $|\dot{S}^{(0)}| \gg |\dot{S}^{(1)}|$, which can be shown to be equivalent to the condition $|\dot{\varepsilon}_k|/\varepsilon_k^2 \ll 1$

The second solution is given by the method of parameter variations,

$$A_2(k,t)(t) = C_{k2} \exp[iS(t)] \int_0^t dt' F_k(t') \exp[-2iS(t')].$$
 (S32)

The constants C_{k1} and C_{k2} can be found if the inequality $|\dot{\varepsilon}_k| \ll \varepsilon_k^2$ holds in the whole time interval during which the drive is turned on. For $F_k(t) \to 0$ for $t \to 0$, we obtain from $A_{00}(k, t = 0) = 1$

$$C_{k1} = 1, \quad C_{k2} = 0, \quad A_{11}(k,t) \approx -\operatorname{sgn} M_k \frac{F_k(t)}{\varepsilon_k(t) + |M_k|} \exp[iS(t)].$$
 (S33)

It is easy to see that Eqs. (S31) and (S33) give the adiabatic results of Eq. (S24). In particular,

$$\langle c_k^{\dagger}(t)c_k(t)\rangle = |A_{11}(k,t)|^2 \to \frac{\varepsilon_k - |M_k|}{2\varepsilon_k},$$
 (S34)

$$\langle c_k^{\dagger}(t)c_{-k}^{\dagger}(t)\rangle = A_{11}^*(k,t)A_{00}(k,t) \to -\frac{F_k(t)\operatorname{sgn} M_k}{2\varepsilon_k(t)}.$$
 (S35)

1. Vicinity of the gap closing for $F_k = 0$

In the topological regime, the WKB condition $\dot{\varepsilon}_k \ll \varepsilon_k^2$ breaks down for small $|M_k|$, i.e., for |k| close to the gapclosing value $|k_\mu| = |\arccos(\mu/2J)|$, which is determined by the condition $\varepsilon_{k_\mu} = 0$ for $F_k = 0$. Formally, for a nonzero M_k , we have $\dot{\varepsilon}_k \propto F_k \dot{F}_k / M_k \to 0$ for $t \to 0$, since $F_k(t) \to 0$ for $t \to 0$. However, already for a small nonzero time, we can have $|M_k| \lesssim |F_k|$ for small $|M_k|$. Then the WKB appoximation requires that $|\dot{\varepsilon}_k| \approx |\dot{F}_k|$ be small compared to $\varepsilon_k^2 \approx F_k^2$; this condition breaks down for small F_k , and thus for a small nonzero time, even if F_k is varying slowly.

For later times, as F_k increases, the condition $|\dot{F}_k| \ll F_k^2$ can be met. Therefore, for small $|M_k|$, the WKB approximation becomes valid for not too small times, when

$$F_k^2(t) \gg |\dot{F}_k(t)|. \tag{S36}$$

The corresponding WKB solution cannot be extended to t = 0, and therefore the constants $C_{k1,2}$ in $A_{11}(k,t)$ are undetermined.

The analysis is simplified if one takes into account that, in the large-time limit, one can expand in Eq. (S32) $S(t') \approx S(t) + (t'-t)\dot{S}$, which gives

$$A_2(k,t) \approx -iC_{k2}(\operatorname{sgn} M_k) \frac{F_k(t)}{2\varepsilon_k(t)} \exp[-iS(t)], \tag{S37}$$

and

$$A_{11}(k,t) \approx -\frac{C_{k1} \exp[iS(t)]}{\varepsilon_k + |M_k|} \left[F_k(t) \operatorname{sgn} M_k - i \frac{\dot{F}_k |M_k|}{2\varepsilon_k^2} \right] - i \frac{C_{k2} \exp[-iS(t)]}{2\varepsilon_k} \left[\varepsilon_k + |M_k| - \frac{F_k \dot{F}_k |M_k|}{\varepsilon_k^2 (\varepsilon_k + |M_k|)} \right]$$
(S38)

In what follows we disregard the terms $\propto \dot{F}_k$ in $A_{11}(k,t)$. We remind that $A_{00}(k,t) = A_1(k,t) + A_2(k,t)$, with $A_{1,2}$ given by Eqs. (S31) and (S37).

The parameters $C_{k1,2}$ can be found by noticing that, quite generally, $F_k(t) \propto t$ for a time that is small, on the one hand but, on the other hand, is sufficiently long, so that $F_k(t)$ becomes large compared to M_k and the above asymptotic expressions for A_{11} , A_{22} apply. We use this to obtain the full WKB solution by matching these expressions to the explicit solution of the Schrödinger equation (S29) for $F_k(t) \propto t$ in terms of the parabolic cylinder functions.

For $F_k(t) = \eta_k t$ and $|\eta_k| t \gg |M_k|$, the condition of the applicability of the WKB approximation $\dot{\varepsilon}_k \ll \varepsilon_k^2$ is reduced to the inequality $|\eta_k| \ll (\eta_k t)^2$. The asymptotic expressions for $A_{00}(k,t)$, $A_{11}(k,t)$ strongly simplify in this case. We

have in these expressions

$$S^{(0)}(t) \approx -\frac{1}{2} |\eta_k| (\operatorname{sgn} M_k) \left\{ t^2 + \frac{M_k^2}{2\eta_k^2} \left[\log(4\eta_k^2 t^2 / M_k^2) + 1 \right] \right\},$$

$$S^{(1)}(t) \approx i \frac{1}{2} \log 2 - i \frac{|M_k|}{2|\eta_k|t}, \quad \varepsilon_k(t) \approx |\eta_k| t \left(1 + \frac{M_k^2}{2\eta_k^2 t^2} \right). \tag{S39}$$

Respectively, the expressions for A_{00} and A_{11} take the form

$$A_{00}(k,t) \approx \frac{C_{k1}}{\sqrt{2}} \left(1 + \frac{|M_k|}{2|\eta_k|t} \right) e^{iS^{(0)}(t)} - i \frac{C_{k2}}{\sqrt{2}} \left(\operatorname{sgn}(M_k \eta_k) - \frac{M_k}{2\eta_k t} \right) e^{-iS^{(0)}(t)},$$

$$A_{11}(k,t) \approx -\frac{C_{k1}}{\sqrt{2}} \left(\operatorname{sgn}(M_k \eta_k) - \frac{M_k}{2\eta_k t} \right) e^{iS^{(0)}(t)} - i \frac{C_{k2}}{\sqrt{2}} \left(1 + \frac{|M_k|}{2|\eta_k|t} \right) e^{-iS^{(0)}(t)}.$$
(S40)

These expressions will be used to match the expansion of the parabolic cylinder functions for $|\eta_k t| \gg |M_k|$. To this end, it is convenient to introduce functions $A_{\pm} = (A_{00} \pm A_{11})/\sqrt{2}$. In particular,

$$A_{-}(k,t) = \begin{cases} C_{k1} \exp(iS^{(0)}) + iC_{k2}(M_k/2\eta_k t) \exp(-iS^{(0)}), & \operatorname{sgn}(M_k \eta_k) = +1 \\ -C_{k1}(M_k/2\eta_k t) \exp(iS^{(0)}) + iC_{k2} \exp(-iS^{(0)}), & \operatorname{sgn}(M_k \eta_k) = -1. \end{cases}$$
(S41)

whereas

$$A_{+}(k,t) = \begin{cases} C_{k1}(M_{k}/2\eta_{k}t) \exp(iS^{(0)}) - iC_{k2} \exp(-iS^{(0)}), & \operatorname{sgn}(M_{k}\eta_{k}) = +1\\ C_{k1} \exp(iS^{(0)}) + iC_{k2}(M_{k}/2\eta_{k}t) \exp(-iS^{(0)}), & \operatorname{sgn}(M_{k}\eta_{k}) = -1. \end{cases}$$
(S42)

Here $S^{(0)} \equiv S^{(0)}(t)$ is given by Eq. (S39).

The parameters $C_{k1,2}$ depend on the ratio M_k^2/η_k . They are found by matching to the parabolic cylinder functions. One can then find A_{00} , A_{11} in the stationary regime, i.e., where $F_k(t)$ has reached its stationary value and no longer varies in time, $\dot{F}_k = 0$. To the first order in M_k/F_k

$$A_{00}(k,t) = \frac{C_{k1}}{\sqrt{2}} e^{iS^{(0)}(t)} \left(1 + \frac{|M_k|}{2|F_k|} \right) - i \frac{C_{k2}}{\sqrt{2}} \operatorname{sgn}(M_k \eta_k) e^{-iS^{(0)}(t)} \left(1 - \frac{|M_k|}{2|F_k|} \right),$$

$$A_{11}(k,t) = -\frac{C_{k1}}{\sqrt{2}} \operatorname{sgn}(M_k \eta_k) e^{iS^{(0)}(t)} \left(1 - \frac{|M_k|}{2|F_k|} \right) - i \frac{C_{k2}}{\sqrt{2}} e^{-iS^{(0)}(t)} \left(1 + \frac{|M_k|}{2|F_k|} \right), \tag{S43}$$

The factors $\exp[\pm iS^{(0)}(t)]$ in these expressions are fast oscillating, and therefore they drop out from the time-averaged parameters

$$\langle |A_{11}(k,t)|^2 \rangle \approx \frac{1}{2} |C_{k1}|^2 \left(1 - \frac{|M_k|}{|F_k|} \right) + \frac{1}{2} |C_{k2}|^2 \left(1 + \frac{|M_k|}{|F_k|} \right),$$

$$\langle A_{11}^*(k,t) A_{00}(k,t) \rangle \approx \frac{1}{2} \left(|C_{k2}|^2 - |C_{k1}|^2 \right)$$
(S44)

These parameters give the correlators we are interested in, cf. Eq. (S34).

B. Solution in terms of the parabolic cylinder functions

For a linear turn-on of the drive, $F_k(t) = \eta_k t$, Eq. (S29) can be solved using the parabolic cylinder functions. Indeed, from Eq. (S29), we obtain the equation for $A_-(t)$, which has the form

$$\frac{d^2 A_{\pm}}{dz_k^2} + \left(s_k \mp \frac{1}{2} - \frac{z_k^2}{4}\right) A_{\pm} = 0, \quad z_k = e^{i(\pi/4)\operatorname{sgn}\eta_k} (2|\eta_k|)^{1/2} t, \quad s_k = -i\frac{M_k^2}{2\eta_k}, \tag{S45}$$

with

$$A_{+} = ie^{i(\pi/4)\operatorname{sgn}\eta_{k}}\operatorname{sgn}M_{k}\left(\frac{dA_{-}}{dz_{k}} + \frac{1}{2}z_{k}A_{-}\right)/|s_{k}|^{1/2}.$$

Equation (S45) is the Weber equation. Its general solution can be expressed in terms of the parabolic cylinder functions,

$$A_{-} = \alpha_{k} D_{-s_{k}-1}(-iz_{k}) + \beta_{k} D_{-s_{k}-1}(iz_{k}),$$

$$A_{+} = \frac{e^{i(\pi/4)\operatorname{sgn} M_{k}} \operatorname{sgn} M_{k}}{\sqrt{|s_{k}|}} \left(-\alpha_{k} D_{-s_{k}}(-iz_{k}) + \beta_{k} D_{-s_{k}}(iz_{k})\right),$$
(S46)

where $D_{\nu}(z)$ are the parabolic cylinder functions [35] and we consider $\pm iz_k \equiv \exp(\pm i\pi/2)z_k$. The factors α_k and β_k are determined by the initial conditions, which gives

$$\alpha_k = \frac{2^{s_k/2}}{\sqrt{4\pi}} \left[\Gamma\left(1 + \frac{s_k}{2}\right) - e^{-i(\pi/4)\operatorname{sgn}\eta_k} \operatorname{sgn} M_k \sqrt{\frac{|s_k|}{2}} \Gamma\left(\frac{1}{2} + \frac{s_k}{2}\right) \right],$$

$$\beta_k = \frac{2^{s_k/2}}{\sqrt{4\pi}} \left[\Gamma\left(1 + \frac{s_k}{2}\right) + e^{-i(\pi/4)\operatorname{sgn}\eta_k} \operatorname{sgn} M_k \sqrt{\frac{|s_k|}{2}} \Gamma\left(\frac{1}{2} + \frac{s_k}{2}\right) \right],$$
(S47)

where $\Gamma(z)$ is the Gamma function.

Equations (S46) and (S47) provide a general solution of the problem of turning on the drive linearly in time at an arbitrary rate η_k for an arbitrary M_k . The solution depends on $z \propto \eta_k t$ and the dimensionless parameter $s_k \propto M_k^2/\eta_k$. It allows us to find the coefficients C_{k1} and C_{k2} , and thus to obtain the full WKB solution of the problem of the two-spin dynamics in the case where the drive is initially turned on linearly in time. This can be done by matching the asymptotic expansion of the solution (S46) in the range $|\eta_k|^{1/2}t \gg 1$ with the Eqs. (S41) and (S42) in the same time range. For completeness, we provide the leading-order terms of the expansion of the parabolic cylinder function $D_{\nu}(z)$ for $|z| \gg 1$, $|\nu|$ [35]:

$$D_{\nu}(z) \approx \begin{cases} e^{-z^{2}/4} z^{\nu}, & |\arg(z)| < 3\pi/4 \\ e^{-z^{2}/4} z^{\nu} - \frac{\sqrt{2\pi}}{\Gamma(-\nu)} e^{i\nu\pi} e^{z^{2}/4} z^{-\nu-1}, & \pi/4 < \arg(z) < 5\pi/4 \\ e^{-z^{2}/4} z^{\nu} - \frac{\sqrt{2\pi}}{\Gamma(-\nu)} e^{-i\nu\pi} e^{z^{2}/4} z^{-\nu-1}, & -5\pi/4 < \arg(z) < -\pi/4. \end{cases}$$
(S48)

We will accept the convention that $\pm iz \equiv z \exp(\pm i\pi/2)$.

We will also use that, from Eqs. (S39) and (S45), in the large-t limit

$$e^{iS_0(t)} \approx e^{-(z_k^2/4)\operatorname{sgn}(M_k\eta_k)} z^{s_k\operatorname{sgn}(M_k\eta_k)} \exp\left[\frac{1}{2}s_k\operatorname{sgn}(M_k\eta_k)\left(-i\frac{\pi}{2}\operatorname{sgn}\eta_k - \log|s_k| + 1\right)\right]$$

whereas

$$\frac{M_k}{2\eta_k t} = \operatorname{sgn}(M_k \eta_k) \frac{\sqrt{|s_k|}}{z_k} e^{i(\pi/4)\operatorname{sgn}\eta_k}$$

To express the parameters of the WKB solution C_{k1} , C_{k2} in terms of the coefficients α_k , β_k of the solution of the equations of motion in terms of the parabolic cylinder functions, it is convenient to introduce auxiliary parameters

$$J_{k} = \frac{\sqrt{2\pi}}{\Gamma(s_{k}+1)} |s_{k}|^{s_{k}/2} \exp\left(-\frac{s_{k}}{2} - \frac{\pi|s_{k}|}{4}\right),$$

$$L_{k} = |s_{k}|^{-(s_{k}+1)/2} \exp\left(\frac{i\pi}{4} \operatorname{sgn} \eta_{k} + \frac{s_{k}}{2} + \frac{\pi|s_{k}|}{4}\right). \tag{S49}$$

In terms of these parameters, from Eqs. (S41), (S42), and (S46) we find that, for $M_k > 0$ and $\eta_k > 0$

$$C_{k1} = \beta_k J_k, \quad C_{k2} = -i \left(\alpha_k - \beta_k e^{-\pi |s_k|} \right) L_k.$$
 (S50)

For $M_k < 0$ and $\eta_k < 0$, on the other hand,

$$C_{k1} = \alpha_k J_k, \quad C_{k2} = -i \left(\beta_k - \alpha_k e^{-\pi |s_k|} \right) L_k. \tag{S51}$$

For $M_k < 0, \eta_k > 0$ we find

$$C_{k1} = \left(\alpha_k - \beta_k e^{-\pi|s_k|}\right) L_k, \quad C_{k2} = -i\beta_k J_k. \tag{S52}$$

For $M_k > 0, \eta_k < 0$ we find

$$C_{k1} = \left(\beta_k - \alpha_k e^{-\pi|s_k|}\right) L_k, \quad C_{k2} = -i\alpha_k J_k. \tag{S53}$$

Equations (S49) - (S53), together with the expressions (S47) for the parameters α_k , β_k provide a complete solution of the problem of the slow turn-on of the drive in the range of zero energy gap in the absence of the drive. The dynamics of the chain depends on a single parameter, the ratio of the squared gap M_k^2 to the rate of the increment of the drive η_k . We note that it is advantageous to express the coefficients C_{k1} , C_{k2} in terms of α_k , β_k , as this allows one to extend the WKB results to different initial conditions.

SM: V. NUMERICAL VALIDATION USING MATRIX PRODUCT STATES

To validate the analytical predictions derived in the thermodynamic limit $(N \to \infty)$, we performed finite-size numerical simulations using the Matrix Product State (MPS) formalism. This approach is exceptionally well-suited for one-dimensional quantum systems with local interactions, such as the spin chain considered here.

A. The Matrix Product State Method

The Hilbert space of a chain of N spins has a dimension that grows exponentially as 2^N . The MPS method resolves this dimensionality problem by efficiently representing a specific class of quantum states, characterized by a limited amount of entanglement. A quantum state of our spin chain can be written as:

$$|\Psi\rangle = \sum_{s_1,\dots,s_N} C_{s_1 s_2 \dots s_N} |s_1 s_2 \dots s_N\rangle \tag{S54}$$

where $s_n = 0, 1$ enumerates the states of the spin at site n and $C_{s_1s_2...s_N}$ is an element of a rank-N tensor with 2^N elements. Following the standard prescription, we decompose this large tensor into a product of smaller rank-3 tensors, one for each site:

$$C_{s_1 s_2 \dots s_N} \approx A_{\alpha_0 \alpha_1}^{s_1} A_{\alpha_1 \alpha_2}^{s_2} \dots A_{\alpha_{N-1} \alpha_0}^{s_N}$$
 (S55)

The maximal value of α_n is called the dimension of bond n. The maximal (over n) bond dimension is usually denoted χ . It determines the maximum amount of entanglement the MPS takes into account, and thus it controls the accuracy of the approximation. The efficiency of MPS stems from the fact that many physically relevant states can be approximated with high fidelity using a bond dimension χ that is significantly smaller than what would be required to represent an arbitrary state in the Hilbert space.

We performed time evolution of an MPS using the *Time-Evolving Block Decimation (TEBD)* algorithm. For our nearest-neighbor Hamiltonian with an even number of sites, we write $\hat{H} = \hat{H}_{\text{even}} + \hat{H}_{\text{odd}}$, where $\hat{H}_{\text{even/odd}} = \sum_{j \in \text{even/odd}} \hat{h}_{j,j+1}$ with $\hat{h}_{j,j+1}$ being the coupling of sites j and j+1. A second-order Trotter decomposition is then:

$$e^{-i\hat{H}\delta t} \approx e^{-i\hat{H}_{\text{odd}}\delta t/2} e^{-i\hat{H}_{\text{even}}\delta t} e^{-i\hat{H}_{\text{odd}}\delta t/2} + \mathcal{O}(\delta t^3).$$

Applying a two-site gate $\exp(-ih_{j\,j+1}\delta t)$ increases the entanglement across the corresponding bond, which would lead to a growth in the required bond dimension. To keep the computation feasible, a truncation step is performed via singular value decomposition (SVD) across a bond, keeping only the χ largest singular values. This step controllably projects the state back into the manifold of states with a manageable bond dimension based on the desired accuracy.

After a quantum quench (sudden change in Hamiltonian parameters), entanglement typically grows linearly in time before it saturates. To maintain accuracy, the bond dimension must grow exponentially with time, which limits the maximum size of the simulated system. For an adiabatic evolution, the entanglement growth is much slower, allowing us to simulate larger systems.

Our simulations were implemented using the ITensor library [36] with a TEBD time-step of $\delta t = 0.1 J^{-1}$ (J = 1 as the unit of energy, $\hbar = 1$). Reflecting the difference in entanglement growth, we used a chain of N = 40 spins for the adiabatic protocols and a smaller chain of N = 20 for the sudden quench protocol.

B. Sudden Quench Simulations

For the sudden quench, the system was initialized in the product state $|\Psi_0\rangle = |\uparrow \dots \uparrow\rangle$ and then evolved under a time-independent Hamiltonian for several values of detuning $\mu \in (0,5)$, separated by a step $\delta\mu = 0.1J$, for a fixed drive amplitude F = 0.5J. The evolution was followed for $0 < t \le t_f = 50J^{-1}$. To compare with the analytical predictions for the time-averaged expectation values, the expectation values of observables were averaged over the time interval from $t = 20J^{-1}$ to $t = 50J^{-1}$.

As discussed in the main text, the analytical results are derived in the thermodynamic limit, whereas our simulations are for finite N. We observe finite-size corrections in our results for the time-averaged nearest-neighbor σ_z correlations. Figure S2 illustrates the deviation of the numerically computed nearest-neighbor correlator $Q^z(1)$ of the increments $\Delta \sigma_n^z$ from the analytical solution. The figure shows that the deviation quickly falls off with the increasing number of sites in the chain.

The scaling of the deviation wih the number of sites can be further quantified by an integrated error $E_N[Q^z(1)] = \int_0^5 d\mu |Q^z(1)_{\infty} - Q^z(1)_N|$, where $Q^z(1)_{\infty}$ is the analytical result and $Q^z(1)_N$ is the simulation result for N sites. As shown in Fig. S3, this error scales as $N^{-1.05}$, confirming that our numerical results agree with the expected scaling of MPS simulations.

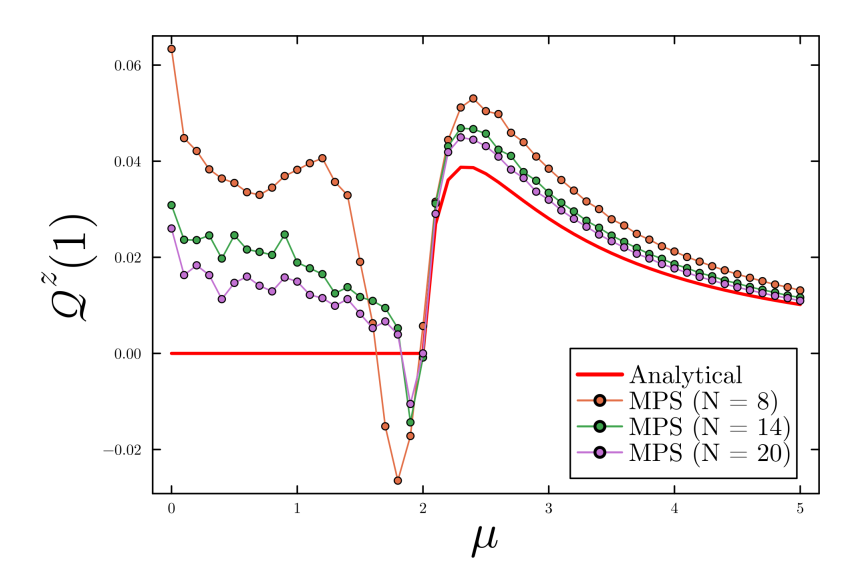


FIG. S2. The time-averaged correlator $Q^z(1)$ for a sudden turn-on of parametric modulation as a function of the scaled frequency detuning μ/J . The final modulation amplitude is F/J=0.5. The analytical result refers to the thermodynamic limit $N\to\infty$.

C. Adiabatic Evolution and Hysteresis

The adiabatic switching protocol was simulated by linearly ramping the drive amplitude as $F(t) = F_f t/\tau_{sl}$ from t=0 to a ramp time of $t_f = \tau_{sl} = 10^3 J^{-1}$, reaching a final amplitude of $F_f = 0.5J$. This was independently performed for the same values of μ as in the sudden quench. After the ramp, the system was evolved with the constant final Hamiltonian for an additional time interval $\Delta t = 30J^{-1}$, over which the time-averaging of observables was performed.

To demonstrate the hysteresis effect, we compare the results described above with the outcome of the following procedure. We switched on the drive amplitude adiabatically to a final value $F_f = 0.5J$ at $t = t_{f_1} = 10^3 J^{-1}$ for $\mu = 5J$ (i.e., in the trivial phase). Then μ was slowly varied as $\mu(t) = J[5 - (t - t_{f_1})/\tau_{\rm sl}]$ from t_{f_1} to $t_{f_1} + 5\tau_{\rm sl}$ with the drive amplitude fixed at $F_f = 0.5J$. his way we accumulated an array of wave functions for the values of $\mu \in (0,4)$ separated by 0.1J. For each of these wave functions the observables of interest were calculated. The system was then evolved for the corresponding μ for a duration $\Delta t = 30J^{-1}$. This allowed us to find the time-averaged values of the

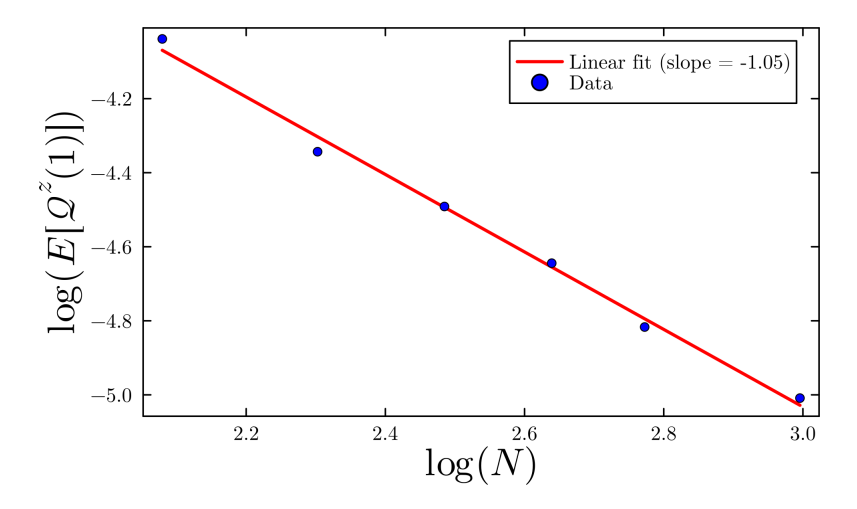


FIG. S3. A log-log plot of the integrated error $E_N[Q^z(1)]$ versus the number of sites N. The linear fit (dashed line) has a slope of approximately -1, confirming that the finite-size corrections to the correlator scale as N^{-1} .

observables plotted in Fig. S1 and in Fig. 3 of the main text.

- [1] H. Suhl, The theory of ferromagnetic resonance at high signal powers, J. Phys. Chem. Solids 1, 209 (1957).
- [2] S. O. Demokritov, V. E. Demidov, O. Dzyapko, G. A. Melkov, A. A. Serga, B. Hillebrands, and A. N. Slavin, Bose–Einstein condensation of quasi-equilibrium magnons at room temperature under pumping, Nature 443, 430 (2006).
- [3] V. S. L'vov, A. Pomyalov, D. A. Bozhko, B. Hillebrands, and A. A. Serga, Correlation-Enhanced Interaction of a Bose-Einstein Condensate with Parametric Magnon Pairs and Virtual Magnons, Phys. Rev. Lett. 131, 156705 (2023).
- [4] J.-Y. Shan, J. B. Curtis, M. Guo, C. J. Roh, C. R. Rotundu, Y. S. Lee, P. Narang, T. W. Noh, E. Demler, and D. Hsieh, Dynamic magnetic phase transition induced by parametric magnon pumping, Phys. Rev. B 109, 054302 (2024).
- [5] D. Malz, J. Knolle, and A. Nunnenkamp, Topological magnon amplification, Nat Commun 10, 3937 (2019).
- [6] M. Arfini, A. Bermejillo-Seco, A. Bondarenko, C. A. Potts, Y. M. Blanter, H. S. J. van der Zant, and G. A. Steele, Magnon-magnon interaction induced by nonlinear spin wave dynamics (2025), arXiv:2506.11527 [cond-mat].
- [7] V. S. L'vov, Wave Turbulence under Parametric Excitation: Applications to Magnets, 1st ed., Springer Series in Nonlinear Dynamics (Springer Berlin, Heidelberg, 2012).
- [8] H. Y. Yuan, Y. Cao, A. Kamra, R. A. Duine, and P. Yan, Quantum magnonics: When magnon spintronics meets quantum information science, Physics Reports 965, 1 (2022).
- [9] T. Holstein and H. Primakoff, Field Dependence of the Intrinsic Domain Magnetization of a Ferromagnet, Phys. Rev. 58, 1098 (1940).
- [10] J. Villain, Quantum-theory of 1- and 2-dimensional ferromagnets and antiferromagnets W an easy magnetization plane. 1. Ideal 1-d or 2-d lattices without in-plane anisotropy, Journal De Physique 35, 27 (1974).
- [11] P. Jordan and E. Wigner, Über das Paulische Äquivalenzverbot, Z. Physik 47, 631 (1928).
- [12] E. Lieb, T. Schultz, and D. Mattis, Two soluble models of an antiferromagnetic chain, Annals of Physics 16, 407 (1961).
- [13] A. Y. Kitaev, Unpaired majorana fermions in quantum wires, Physics-Uspekhi 44, 131 (2001).
- [14] M. Thakurathi, A. A. Patel, D. Sen, and A. Dutta, Floquet generation of majorana end modes and topological invariants, Phys. Rev. B 88, 155133 (2013).
- [15] D. J. Yates, F. H. L. Essler, and A. Mitra, Almost strong 0, \$\pi\$ edge modes in clean, interacting 1D floquet systems, Phys. Rev. B **99**, 205419 (2019).
- [16] E. Vernier, H.-C. Yeh, L. Piroli, and A. Mitra, Strong Zero Modes in Integrable Quantum Circuits, Phys. Rev. Lett. 133, 050606 (2024).
- [17] N. Tausendpfund, A. Mitra, and M. Rizzi, Almost strong zero modes at finite temperature, Phys. Rev. Res. 7, 023245 (2025).
- [18] X. Mi et al., Noise-resilient edge modes on a chain of superconducting qubits, Science 378, 785 (2022).
- [19] H. Schmid, A.-G. Penner, K. Yang, L. Glazman, and F. von Oppen, Robust Spectral \ensuremath{\pi}\\$ Pairing in the Random-Field Floquet Quantum Ising Model, Phys. Rev. Lett. 132, 210401 (2024).
- [20] F. Jin et al., Topological prethermal strong zero modes on superconducting processors, Nature 645, 626 (2025).
- [21] M. I. Dykman, Coherent multiple-period states of periodically modulated qubits, Phys. Rev. A 100, 042101 (2019).
- [22] Y. Liang, W. Huang, L. Zhang, Z. Tao, K. Tang, J. Chu, J. Qiu, X. Sun, Y. Zhou, J. Zhang, J. Zhang, W. Guo, Y. Liu, Y. Chen, S. Liu, Y. Zhong, J. Niu, and D. Yu, Floquet engineering of anisotropic transverse interactions in superconducting

- qubits (2024), arXiv:2410.10208.
- [23] See Supplemental Material, which provides details of the calculations in the main text.
- [24] G. Zhang and Z. Song, Topological Characterization of Extended Quantum Ising Models, Phys. Rev. Lett. 115, 177204 (2015).
- [25] Q.-G. Liu, H.-G. Cheng, S. Qu, B. Guo, and Z.-Y. Sun, Multipartite nonlocality spectrum and topological quantum phase transitions in a one-dimensional extended quantum Ising model, Physics Letters A 557, 130858 (2025).
- [26] Y. B. Shi, K. L. Zhang, and Z. Song, Dynamic generation of nonequilibrium superconducting states in Kitaev chain, Phys. Rev. B 106, 184505 (2022).
- [27] C. P. Slichter, Principles of Magnetic Resonance (Springer, Berlin, 1990).
- [28] A. Blais, A. L. Grimsmo, S. M. Girvin, and A. Wallraff, Circuit quantum electrodynamics, Rev. Mod. Phys. 93, 025005 (2021).
- [29] J. Dziarmaga, Dynamics of a quantum phase transition: Exact solution of the quantum ising model, Phys. Rev. Lett. 95, 245701 (2005); Dynamics of a quantum phase transition and relaxation to a steady state, Adv. Phys. 59, 1063 (2010).
- [30] K. Polkovnikov, A.and Sengupta, A. Silva, and M. Vengalattore, Colloquium: Nonequilibrium dynamics of closed interacting quantum systems, Rev. Mod. Phys. 83, 863 (2011).
- [31] P. Calabrese, F. H. L. Essler, and M. Fagotti, Quantum quench in the transverse field Ising chain: I. Time evolution of order parameter correlators, J. Stat. Mech. 2012, P07016 (2012).
- [32] M. Heyl, Dynamical Quantum Phase Transitions in the Transverse-Field Ising Model, Phys. Rev. Lett. 110, 135704 (2013).
- [33] A. Grabarits, F. Balducci, and A. del Campo, Driving a quantum phase transition at an arbitrary rate: Exact solution of the transverse-field Ising model, Phys. Rev. A 111, 042207 (2025).
- [34] Editorial, Spins in chains, Nature Materials 24, 651 (2025).
- [35] I. S. Gradshteyn and I. M. Ryzhik, Tables of Integrals, Series and Products, 8th ed. (Elsevier, Amsterdam, 2015).
- [36] M. Fishman, S. R. White, and E. M. Stoudenmire, The ITensor Software Library for Tensor Network Calculations (2021), arXiv:2007.14822 [cs].